Structural and functional analysis of Nup133 domains reveals modular building blocks of the nuclear pore complex

Ian C. Berke, Thomas Boehmer, Günter Blobel, and Thomas U. Schwartz

Laboratory of Cell Biology, Howard Hughes Medical Institute, The Rockefeller University, New York, NY 10021

Nucleocytoplasmic transport occurs through nuclear pore complexes (NPCs) whose complex architecture is generated from a set of only ~30 proteins, termed nucleoporins. Here, we explore the domain structure of Nup133, a nucleoporin in a conserved NPC subcomplex that is crucial for NPC biogenesis and is believed to form part of the NPC scaffold. We show that human Nup133 contains two domains: a COOH-terminal domain responsible for its interaction with its subcomplex through Nup107; and an NH_2-terminal domain whose crystal structure reveals a seven-bladed β-propeller. The surface properties and conservation of the Nup133 β-propeller suggest it may mediate multiple interactions with other proteins. Other β-propellers are predicted in a third of all nucleoporins. These and several other repeat-based motifs appear to be major elements of nucleoporins, indicating a level of structural repetition that may conceptually simplify the assembly and disassembly of this huge protein complex.

Introduction

Macromolecular exchange between the cytoplasm and nucleus is a vital process involving a mobile phase of transport proteins and regulatory factors, and a stationary phase comprised of nuclear pore complexes (NPCs) embedded in the nuclear envelope (NE). Structural studies of mobile phase components have revealed the molecular details of cargo binding, regulation by Ran GTPase, and how transport factors interact with the NPC (Chook and Blobel, 2001), but the enormity of the stationary phase of nucleocytoplasmic transport has so far frustrated such efforts. Nonetheless, a low-resolution picture of the NPC and its organization is emerging. NPCs have a conserved eightfold symmetric framework with peripheral fiberlike extensions into both the cytoplasm and nucleus (Suntharalingam and Wente, 2003). An NPC has an estimated mass of 125 MD in vertebrates and 55–72 MD in yeast, yet is comprised of only ~30 proteins termed nucleoporins (Rout et al., 2000; Cronshaw et al., 2002). Nucleoporins are organized in subcomplexes that can be isolated from mitotic extracts or through biochemical extraction of the NE. These modular units are present in multiple copies arranged around two- and eightfold axes of symmetry and are believed to generate discrete structures within the NPC (Suntharalingam and Wente, 2003).

The nonameric Nup107-160 subcomplex in vertebrates (Loiodice et al., 2004) forms part of the peripheral circular core structure of the NPC and is located in close vicinity to the sharp bend between the outer and inner nuclear membranes (Belgareh et al., 2001). Immunodepletion of this subcomplex from *Xenopus laevis* egg extracts prevents reformation of even partial NPCs in nuclear reconstitution assays (Harel et al., 2003; Walther et al., 2003). Targeted depletion of Nup107 by RNA interference prevents integration of the subcomplex member Nup133, but allows other proteins of the subcomplex to be incorporated. Nup107-depleted NPCs were slightly compromised in their ability to export mRNA but did not affect the overall growth rate of cells (Boehmer et al., 2003; Galy et al., 2003; see, however, Walther et al., 2003).

In yeast, the homologous heptameric Nup84 subcomplex has been assembled in vitro from recombinant dimers and trimers produced in *Escherichia coli* (Lutzmann et al., 2002). By negative staining electron microscopy, the subcomplex has a Y-shaped structure with Nup133 located at the base of the stalk and Nup84 (the yeast homologue of Nup107) being its nearest neighbor. Nup133 depletion in yeast causes temperature-sensitive growth and mRNA export defects and clustering of NPCs at one pole of the NE (Doye et al., 1994; Pemberton et al., 1995).

Although an essentially complete inventory of nucleoporins is at hand and their organization into subcomplexes estab-

The online version of this article includes supplemental material.

Correspondence to Günter Blobel: blobel@rockefeller.edu

T.U. Schwartz's present address is Dept. of Biology, Massachusetts Institute of Technology, Cambridge, MA 02139.

Abbreviations used in this paper: CTD, COOH-terminal domain; NE, nuclear envelope; NPC, nuclear pore complex; NTD, NH_2-terminal domain.

The Journal of Cell Biology, Vol. 167, No. 4, November 22, 2004 591–597
http://www.jcb.org/cgi/doi/10.1083/jcb.200408109

lished, little information is available about the structural details of NPC architecture. Except for a 160-residue COOH-terminal fragment of Nup98 (Hodel et al., 2002), there is no other atomic structure of a nucleoporin available. Nup98 has been proposed to be a "mobile" nucleoporin from studies with GFP-tagged protein and FRAP experiments (Griffis et al., 2002). In contrast, members of the Nup107-160 subcomplex are stably associated with the NPC during interphase (Belgareh et al., 2001). Given the importance of this subcomplex in NPC assembly, its stability and its Y-shaped structure, the Nup107-160 subcomplex and its homologues have been proposed to form a portion of the central scaffold of the NPC (Belgareh et al., 2001; Harel et al., 2003). Here, we show the subcomplex member Nup133 contains two domains: a COOH-terminal domain (CTD) that anchors Nup133 via Nup107 to its subcomplex, and an NH_2-terminal domain (NTD) that folds into a seven-bladed β-propeller structure determined crystallographically at 2.35 Å. The discovery of a β-propeller domain unexpected by sequence analysis prompted us to examine other nucleoporins for this fold. Candidate β-propeller domains were found in three nucleoporins in addition to the six previously identified by their sequence repeats (Table I). High symmetry, modular subcomplexes built from a small component set, and high frequency of some structural modules show that the high degree of complexity in NPC organization is generated from multiple levels of modularity.

Results and discussion

Nup133 contains two structural domains

Examination of the 1,156-residue human Nup133 by secondary structure prediction, disordered region prediction, and sequence conservation among homologues identified two domains: an NH_2-terminal α/β domain of ~400 residues and an all helical CTD of ~640 residues (Fig. 1 a). Reconstitution of recombinant yeast Nup84 subcomplex revealed that Nup133 is anchored to the subcomplex via its direct interaction with Nup84, the yeast homologue of Nup107 (Lutzmann et al., 2002). Accordingly, Nup133 failed to assemble into NPCs of vertebrate cells depleted of Nup107 (Boehmer et al., 2003). In vitro binding experiments, performed with recombinant GST-Nup107 and in vitro transcribed and translated Nup133 proteins, show that the Nup133 CTD binds Nup107 (Fig. 1 b). GFP-tagged hNup133 (502–1156) shows punctate nuclear rim staining consistent with integration into the Nup107-160 subcomplex and the NPC (Fig. 1 c).

In yeast two-hybrid screens using Nup133 as bait, the extreme COOH terminus of hNup107 was sufficient for their interaction (Belgareh et al., 2001), suggesting Nup133 and Nup107 interact in a tail-to-tail fashion. Nup133 is an elongated and curved molecule at the base of the yeast Y-shaped Nup84 assembly (Lutzmann et al., 2002). Given this shape and the tail-to-tail interaction with Nup107, the Nup133 NTD may

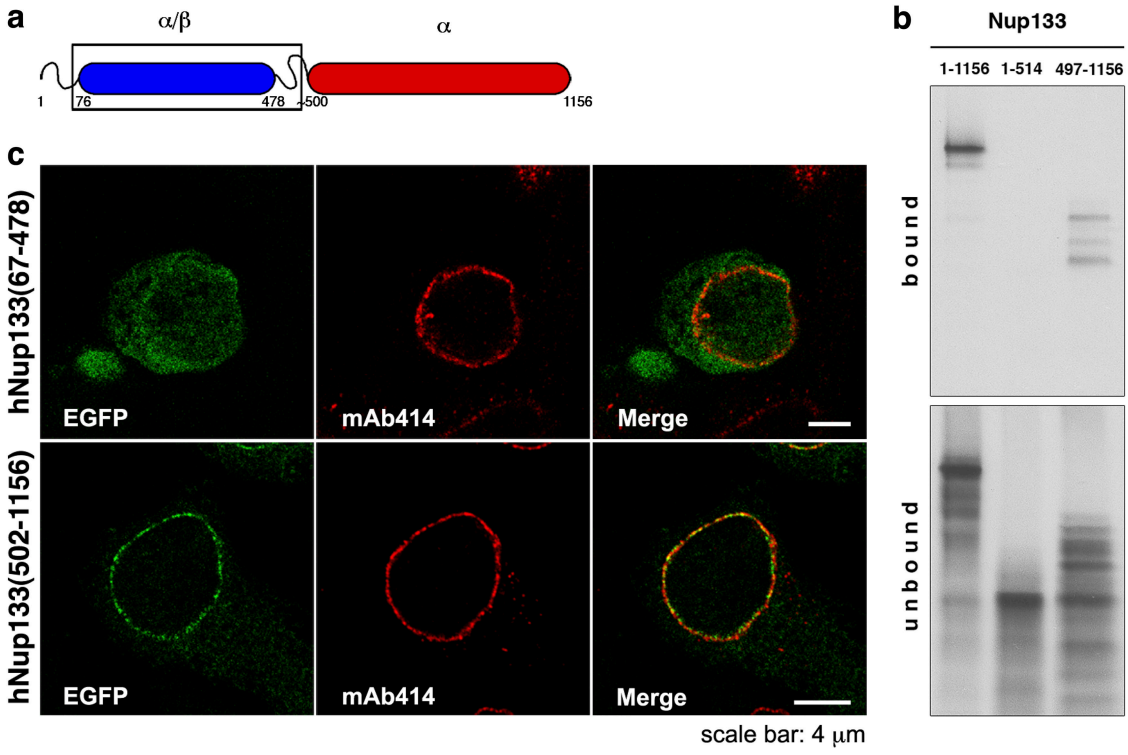

Figure 1. **Domain structure of Nup133.** (a) Two domains were predicted, with the NTD having helical and sheet content, and the CTD being all helical. The construct used for crystallization is boxed. (b) In vitro binding of hNup133 domains to recombinant GST-hNup107. Top and bottom panels show the bound and unbound fractions of various [^{35}S]methionine-labeled Nup133 translation products incubated with recombinant GST-Nup107 immobilized on affinity resin. (c) Localization of EGFP-tagged hNup133 domains in HeLa cells. The CTD shows punctate rim staining that overlaps with the mAb414 signal. The NTD shows diffuse EGFP-signal, with a weak concentration at the nuclear rim.

be positioned at the very end of the Nup107-160 subcomplex, allowing it to mediate interactions to adjoining nucleoporins or associated proteins. Experiments that prevent Nup133 incorporation by depleting its nearest neighbor Nup107 cause a subset of peripheral nucleoporins (Nup153, Nup214, Nup358, and TPR) to be depleted, whereas more centrally located nucleoporins are not affected (Boehmer et al., 2003). GFP-tagged hNup133 (67–478) in HeLa cells is dispersed throughout the cell with a slight concentration at the nuclear rim (Fig. 1 c). If the unknown NTD binding sites are of low affinity, dynamic binding of the overexpressed GFP-NTD would result in an equilibrium between NPCs, cytoplasmic and nucleoplasmic pools, and the dispersed staining observed (Fig. 1 c). Competition with endogenous NTDs tethered to the NPC via their CTDs would further reduce nuclear rim staining. In yeast, Nup133 containing a deletion in the NTD complements RNA export and temperature-sensitive growth defects of Nup133 null mutants, but not an NPC clustering phenotype (Doye et al., 1994). Therefore, the Nup133 NTD may be involved in mediating interactions whose disruption compromises yeast NPC distribution.

Structure of the Nup133 NTD reveals a β-propeller fold

We expressed the NTD of hNup133 (residues 67–514) in *E. coli*, crystallized it, and solved the structure to 2.35 Å. hNup133 NTD is a β-propeller with seven, four-stranded β-sheets arranged face to face around a central water-filled cavity (Fig. 2, a and b; and Video 1, available at http://www.jcb.org/cgi/content/full/jcb.200408109/DC1). The polypeptide chain enters each propeller blade from the innermost strand and folds in an antiparallel manner (Fig. 2 a and Fig. 3 a, strands labeled A–D). Blade 7 of the propeller consists of the innermost three strands from the COOH terminus with the blade completed by the NH_2 terminus of the domain. This 3 + 1 molecular clasp architecture is a common feature for stabilizing β-propellers (Paoli, 2001). The repeating antiparallel structure results in a top surface composed of the loops connecting strand D of one blade to strand A of the next (DA loop) as well as the BC loop within each blade, whereas the bottom surface is composed of the AB and CD loops. Two significant α-helical insertions are present in DA loops (Fig. 2, a and b, pink). The α1 helix inserts between the interface of blades 7 and 1, displacing blade 7 away and blade 1 toward the central axis. Blade 5 is extended and curls around helix α2 located in the DA loop connecting blades 4 and 5. This helical "wing" juts out from the core of the propeller by 15 Å. A disordered 20-residue insertion is present in the DA loop connecting blades 3 and 4 (DA_{34}). The propeller has an overall diameter of 45–50 Å and the β-sheet core is ~25-Å thick. Blade 2 has a short 3_{10} helix just before strand 2A that projects into the top of the inner channel (Fig. 2 a; and Fig. 3 a, orange) and strand 2A is oriented away from the pseudo-

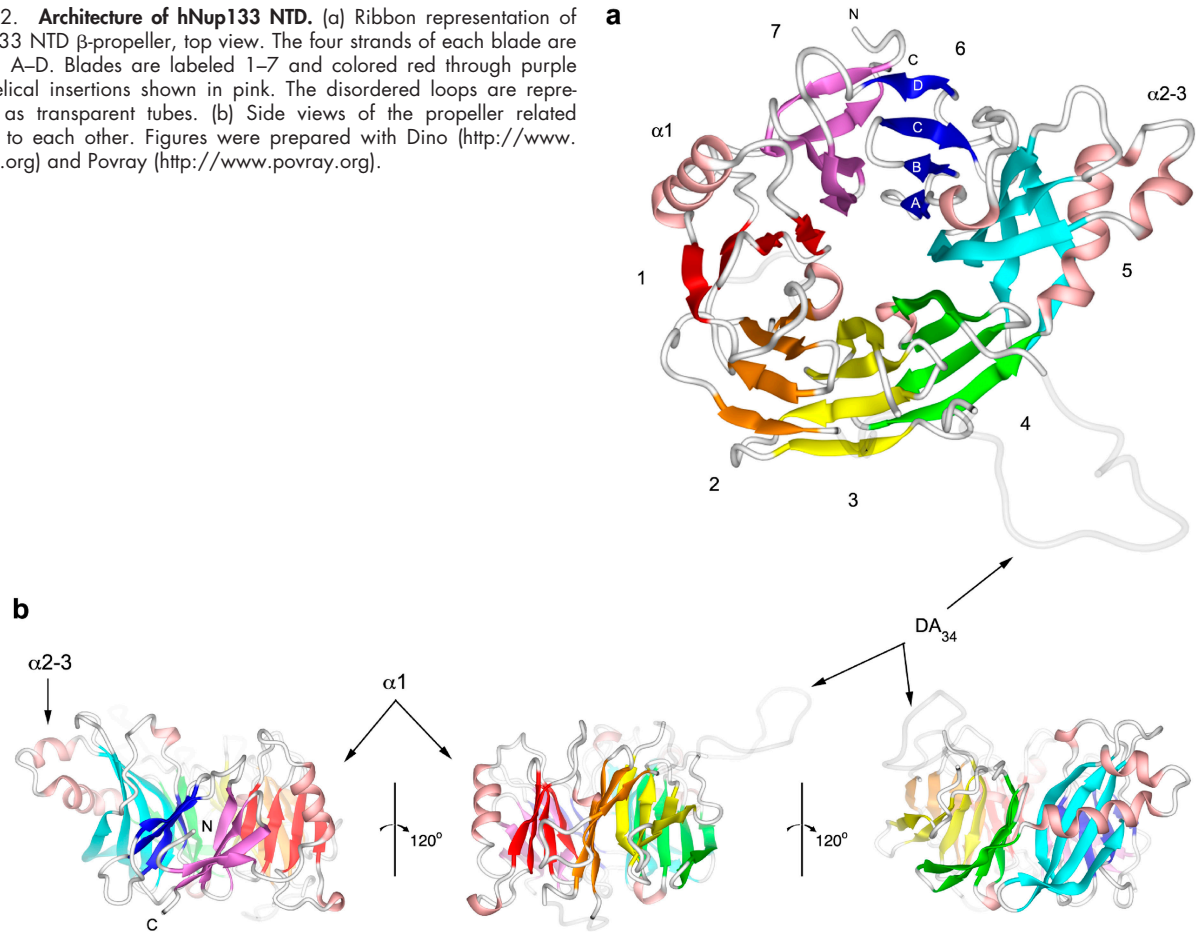

Figure 2. **Architecture of hNup133 NTD.** (a) Ribbon representation of hNup133 NTD β-propeller, top view. The four strands of each blade are labeled A–D. Blades are labeled 1–7 and colored red through purple with helical insertions shown in pink. The disordered loops are represented as transparent tubes. (b) Side views of the propeller related ~120° to each other. Figures were prepared with Dino (http://www.dino3d.org) and Povray (http://www.povray.org).

sevenfold axis such that the bottom of the channel is wider than the top. The inner channel is oval shaped, being 12–16 Å wide at the top and 12–20 Å at the bottom (C_α to C_α), and contains many ordered water molecules.

β-Propellers are repeat proteins believed to have evolved multiple times by gene duplication and fusion of proto-40–50-residue β-sheets (Paoli, 2001). Support for this hypothesis comes from the existence of 4-, 5-, 6-, 7-, and 8-bladed propellers, their wide distribution in function and phylogeny, and the existence of sequence repeats within some of these proteins. Structural alignment of each blade from hNup133 NTD shows no absolutely conserved residues (Fig. 3 c). The blades superimpose very well with a root mean squared deviation of 1.29 Å over 21 aligned C_α atoms (Fig. 3, a and b, spheres). The sequence pattern of strand B is the most conserved, with a hydrophobic core flanked on both sides by polar residues stabilizing the AB and BC loops by hydrogen bonding to the peptide backbone or to a neighboring blade. The tight β-turn in the BC loop is conserved except for the extended blade 5 that contains two sequential turns in its loop (Fig. 3, a and b, cyan). Though more variable than the BC loop, the AB loop also tends to be short with the exception of the flexible AB loop of blade 2 (Fig. 3 b, orange). As in most propellers, strand D is the most variable in length and sequence (Paoli, 2001) and most notably strand 7D has an irregular bulge that contributes to the packing interface between blade 7, α1, blade 1, and its CD loop (Fig. 2 b, left; and Fig. 3 a, purple). A Dali search for the nearest structural homologues revealed that Tup1, transducin, and clathrin NTD β-propellers align with root mean squared deviations of 3.5, 3.4, and 3.9 Å over 278, 272, and 278 C_α atom, respectively. Tup1 and transducin are WD-repeat propellers characterized by an electrostatic network of residues (D-H-S-W) that stabilize the strands within a blade (Paoli, 2001). No such networks are found in the Nup133 NTD propeller, and the Trp-Asp residues at the end of strand C that WD repeats are named for are not conserved. The sequence of Nup133 NTD blades appear more like that of clathrin NTD blades (ter Haar et al., 1998), with mainly a pattern of hydrophobic residues marking the repeats (Fig. 3 c).

Conserved features suggest multiple interactions and a regulatable interaction motif

Proteins with the β-propeller fold have diverse functions ranging from catalysis, intra- and extracellular signaling, vesicular sorting, and DNA binding (Paoli, 2001). The wide range of functional possibilities for this fold reflects the variety of interaction surfaces in the β-propeller scaffold: top and bottom surfaces are composed of variable loops that can serve as a docking platform for other proteins; the side surface is composed of

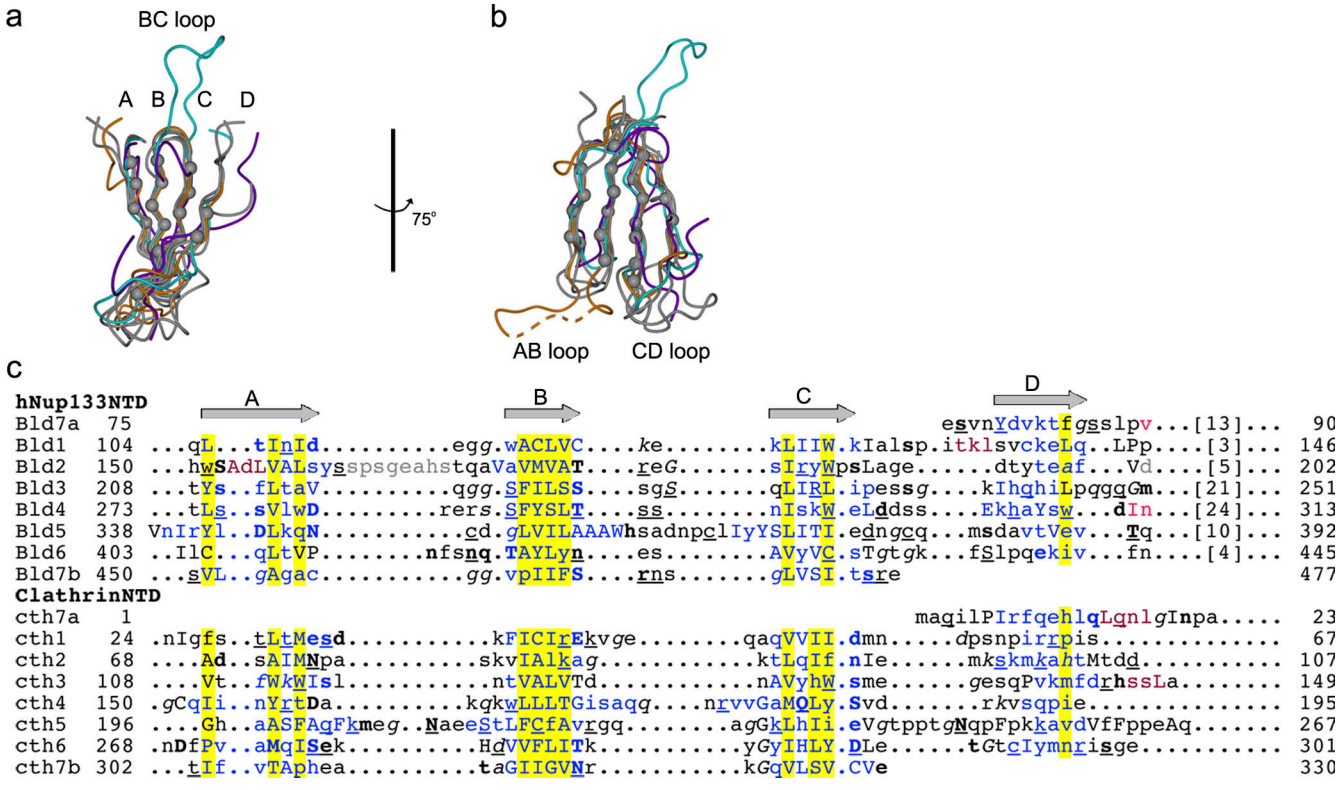

Figure 3. **Structural alignment of the seven blades in the Nup133 β-propeller.** (a and b) Superposition of 21 C_α positions from each blade calculated by the program MultiProt (http://bioinfo3d.cs.tau.ac.il/MultiProt/). Gray spheres mark the aligned C_α atoms from blade 3. Strand A lines the inner channel of the propeller and is roughly parallel to the pseudo-sevenfold axis. Blade 2 (orange), blade 5 (cyan), and blade 7 (purple) contain insertions. (c) Structure-based sequence alignment of Nup133 NTD blades. Conserved hydrophobic positions are shaded yellow. Clathrin NTD propeller blades are shown for comparison. The sequence is shown in Joy formatting (http://www-cryst.bioc.cam.ac.uk/~joy/). β-Strands are shown in blue, 3_{10} helices are shown in maroon, capitalized residues are solvent inaccessible, bold indicates a sidechain-backbone amide H-bond, underline indicates sidechain-backbone carbonyl H-bond, and italics indicates a residue with positive phi values. Gray residues were not built in the model. Bracketed numbers refer to residues not depicted.

grooves at the β-sheet interfaces often involved in peptide interactions; and the inner cavity potentially provides a space for sequestering ligands from bulk solvent. The lack of structural constraints on the evolution of a β-propeller's primary sequence makes this an extremely adaptable module. Mapping the conservation of Nup133 NTDs from six vertebrate species, two insects, and two worms on the hNup133 propeller surface reveals conserved patches that extend along its circumference from blade 5 through blade 2 (Fig. 4 a, left and middle; and Fig. S1, alignment, available at http://www.jcb.org/cgi/content/full/jcb.200408109/DC1). The interface between blade 5 and α2-3 forms a conserved groove that is flanked at either end by negative charges (Fig. 4, a and b). The strongest surface conservation is centered on the α1 insert and a conserved hydrophobic groove runs between α1 and blade 7 (Fig. 4 a). Rotating around the pseudo-sevenfold axis of the propeller, a long disordered but conserved loop (DA_{34}) follows strand 3D (Fig. 4 a, tube representation; and Fig. 4 c, sequence alignment). The loop lies above the entrance to a pocket in the interface between blades 3 and 4 (Fig. 4 b, right).

A common theme shared by many β-propeller domains is their ability to organize dynamic multiprotein complexes. Clathrin forms cages around budding vesicles with their β-propellers recruiting cargo and adaptor complexes, resulting in a supramolecular coat over the membrane (ter Haar et al., 2000; Miele et al., 2004). As in clathrin, the Nup133 β-propeller is attached to a structural scaffold. The most conserved patches of residues in the Nup133 β-propeller (Fig. 4 a, left and middle) are located at some distance from one another and may participate in separate peptide-in-groove interactions similar to the clathrin box motif association with clathrin NTD (ter Haar et al., 2000). Moreover, the high conservation of the DA_{34} loop suggests it has a functional role in interacting with other proteins even though it is disordered. An emerging paradigm in the regulation of protein interactions is the importance of disordered regions that become ordered upon binding (Dunker et al., 2002). Disorder–order transitions allow low affinity and high specificity interactions and regulation of binding through post-translational modifications such as phosphorylation. The loop contains a protein kinase A consensus site that is conserved

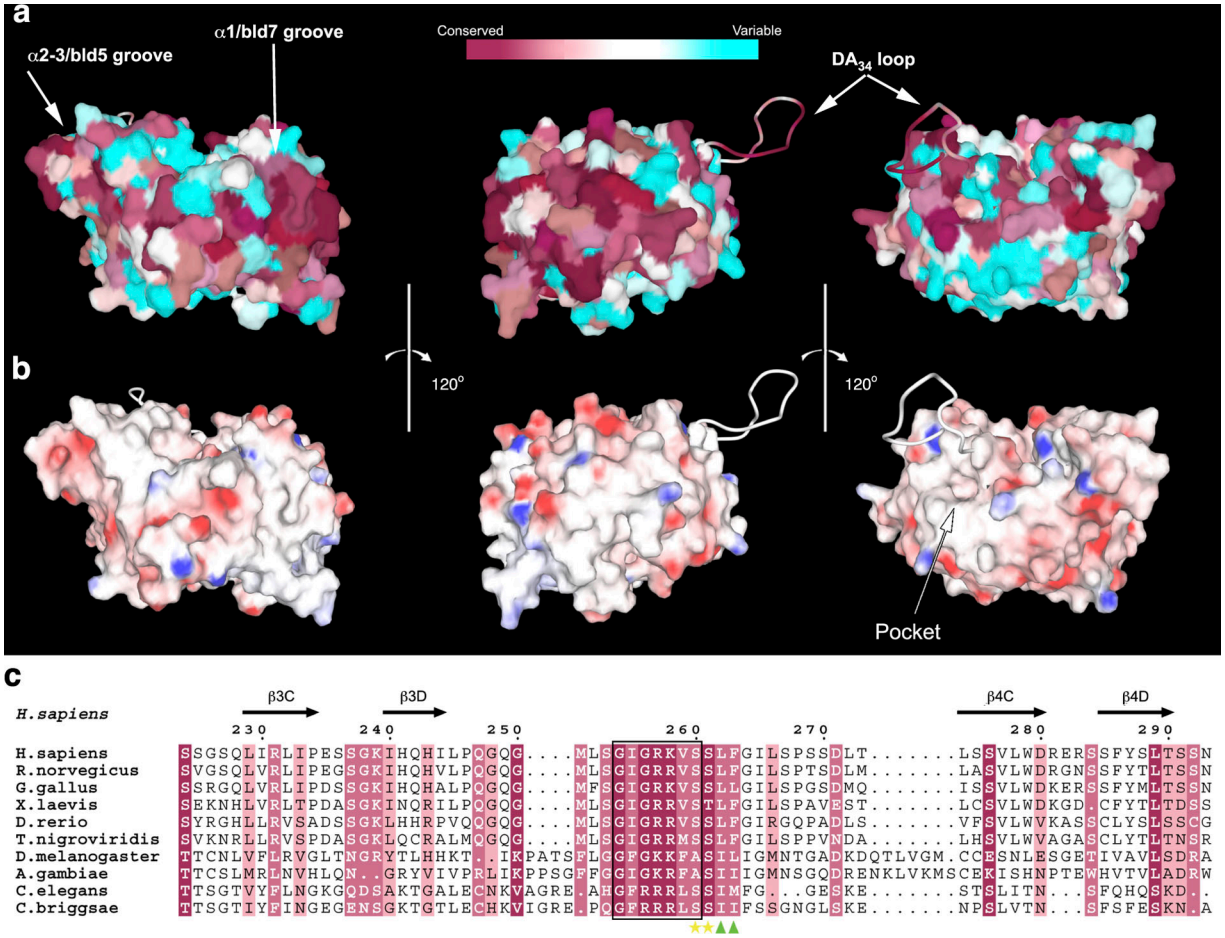

Figure 4. **Conserved features of the Nup133 NTD propeller.** (a) Surface representation showing conservation of residues on the propeller sides. Each view is an ~120° rotation about the pseudo-sevenfold axis beginning from the NH_2 and COOH termini in blade 7 and is the same as in Fig. 2 b. The tube marks the region of the disordered DA_{34} loop. Conservation scores were calculated using the ConSurf Server (http://consurf.tau.ac.il/) and colored maroon (most conserved) to cyan (most variable). (b) Electrostatic potential of the Nup133 β-propeller. Orientation is as in part a. Red indicates negative regions of the potential and blue indicates positive regions. (c) Sequence alignment of the DA_{34} loop across representative metazoans. Position of the conserved protein kinase A consensus site is boxed and potential phosphorylated residues are marked by yellow stars. Green triangles mark conserved hydrophobic positions.

among metazoans (Fig. 4 c, boxed residues) and two conserved serines (Fig. 4 c, yellow stars) are located just before conserved hydrophobic residues (Fig. 4 c, green triangles). Phosphorylation of nucleoporins affects their disassembly during open mitosis (Macaulay et al., 1995; Favreau et al., 1996). Interestingly, fungi, which do not undergo an open mitosis, do not have conserved serines or threonines in this region of Nup133 (Fig. S1).

Modularity of the NPC

NPC organization seems to be simplified at several structural levels. At the multiprotein level, a high degree of symmetry reduces the number of proteins required to generate such a large complex. In addition, these proteins are organized into modular subcomplexes, simplifying the number of interactions that need to be regulated for NPC assembly and disassembly to just those that mediate inter-subcomplex association. The structural modularity of Nup133 and the unexpected finding of a β-propeller domain in it led us to examine other nucleoporins. Fold recognition algorithms predict β-propellers in nine additional nucleoporins (Table I), making this domain a common module of the NPC. Systems specific to eukaryotes have been shown to be enriched in proteins derived from repeating elements (Marcotte et al., 1999), and other repeat modules are predicted or known to exist in the NPC including coiled-coils (Bailer et al., 2001), helical-solenoid–forming repeats (Devos et al., 2004), and phenylalanine-glycine sequence repeats. Each class of repeat provides a scaffold with advantages for different modes of interaction (Andrade et al., 2001): helical solenoids have a large solvent-accessible surface well suited for large or tandem protein interfaces; coiled-coils are excellent mediators of oligomerization; compact, stable repeat structures such as β-propellers are ideal for forming reversible interactions with several partners; and phenylalanine-glycine repeats provide disordered peptides for low-affinity, high-specificity interactions with karyopherins. Before the proteomic analysis of the yeast and vertebrate NPCs, it was estimated that at least 100 nucleoporins existed. In much the same way as the true component set was found to be simplified, perhaps the set of structural motifs within the NPC is also more basic, with a limited set of repeat modules mixed and matched to generate the startling structural and dynamic complexity observed.

Table I. **Nucleoporins containing β-propeller domains**

Nucleoporin	Residues	References
Nup107-160 complex		
Nup133	76–478	
Nup160 (yNup120)		Devos et al., 2004
Sec13[b]		Cronshaw et al., 2002
Seh1[b]		Cronshaw et al., 2002
Nup37[b,c]		Cronshaw et al., 2002
Nup43[b,c]		Cronshaw et al., 2002
Nup214 complex		
Nup214 (yNup159)[a]	1–455	
Nup88 (yNup82)[a]	50–550	
Other		
Aladin[b,c]		Cronshaw et al., 2002
Nup155 (yNup170)[a]	50–550	

[a]400–500-residue domains predicted to contain mostly β-sheet structure were submitted to the SAM-T02 server (HMM based; http://www.cse.ucsc.edu/research/compbio/HMM-apps/T02-query.html) and Fugue Server (environment specific score matrices; http://www-cryst.bioc.cam.ac.uk/~fugue/prfsearch.html) for fold prediction.
[b]WD-repeat protein.
[c]No yeast homologue identified.

Materials and methods

Sequence analysis
Secondary structure prediction of human Nup133 was performed with the PredictProtein server (http://cubic.bioc.columbia.edu/predictprotein), disordered region prediction with Pondr (http://www.pondr.com), and multiple alignment of homologous Nup133 sequences with ClustalW. Regions of secondary structure and homology separated by disordered, nonhomologous regions of >40 amino acids were considered separate domains.

In vitro binding assays
Full-length and mutant Nup133 proteins (amino acids 1–1156, 1–514, and 497–1156) were in vitro transcribed and translated in the presence of [^{35}S]methionine by a coupled reticulocyte lysate transcription/translation system (TNT T7; Promega). Binding assays were performed essentially as described previously (Yaseen and Blobel, 1999) using recombinant full-length Nup107 fused to GST and in vitro transcribed/translated Nup133 proteins as indicated in the figure legends. Bound and unbound fractions were resolved by SDS-PAGE and analyzed by autoradiography.

Transfection and immunofluorescence microscopy
HeLa cells were grown in DME (Invitrogen) supplemented with 10% FBS, penicillin, and streptomycin. For transfections and immunofluorescence microscopy, cells were grown on coverslips and transfected using Effectene (QIAGEN) following the manufacturer's instructions. 24 h later, cells were washed twice with PBS and fixed/permeabilized in 100% methanol at −20°C for 5 min. Costaining with mAb414 (BAbCO) was performed as described previously (Boehmer et al., 2003) except that CY5-conjugated donkey α–mouse IgG antibodies (Jackson ImmunoResearch Laboratories) were used as secondary antibodies. Samples were examined using a spectral confocal microscope (model TCS SP; Leica). Images were processed in Adobe Photoshop CS.

Protein preparation and crystallization
Residues 67–514 of human Nup133 with a His_6 tag and thrombin cleavage site at the NH_2 terminus were expressed in *E. coli* strain BL21 CodonPlus(DE3)-RIL cells at 23°C. Nup133 NTD was purified using a nickel affinity resin followed by thrombin cleavage overnight. The protein was further purified on a HiTrap Q anionic exchange column and gel filtration on a Superdex 75 column. Before crystallization, hNup133 NTD was concentrated to 10 mg ml^{-1} in 20 mM Tris-Cl, pH 8.0, 150 mM NaCl, and 3 mM dithiothreitol. The protein was crystallized at 4°C with the hanging drop vapor diffusion method by mixing 2.5 μl of protein with 2.5 μl of precipitant solution, containing 17–19% (wt/vol) PEG 3350, 100 mM Bis-Tris, pH 5.6–6.2, and 200 mM Li_2SO_4. Crystals were cryo protected in paraffin oil and frozen in liquid N_2. Selenomethionine-substituted derivatives were prepared according to published protocols (Doublie, 1997).

Data collection, structure determination, and refinement
A SAD data set (to 2.5 Å) of an SeMet derivative was collected at 100 K at the 8.2.1 beamline of the Advanced Light Source. Two selenium sites (out of five possible) were identified with the program Shake-and-Bake (Weeks and Miller, 1999) and an additional two sites were found using the program SHARP (de la Fortelle and Bricogne, 1997). The resulting solvent-flattened electron density map was used to build an initial model that was refined using CNS (Brunger et al., 1998) and REFMAC5. The resulting model was refined against native data collected to 2.35 Å. The quality of the final model was validated using the program PROCHECK of the CCP4 suite (Collaborative Computational Project Number, 1994) and contains residues 75–162, 170–201, 206–251, and 270–477 and 97 water molecules. Coordinates and native structure factors were submitted to the Protein Data Bank with accession code 1XKS. Final statistics are provided in Table S1 (available at http://www.jcb.org/cgi/content/full/jcb.200408109/DC1).

Online supplemental material
Data and refinement statistics for the determination of hNup133 NTD are provided in Table S1. Video 1 shows the hNup133 β-propeller rotating top to bottom, and then around its circumference. A multiple sequence alignment of Nup133 NTDs across representative vertebrates, insects,

worms, and fungi is provided in Fig. S1. Online supplemental material is available at http://www.jcb.org/cgi/content/full/jcb.200408109/DC1.

We thank J. Glavy for advice and discussion, members of the Blobel laboratory for assistance and knowledge shared during this project, M. Rout for stimulating discussions and comments, and the staff at Advanced Light Source beamline 8.2.1 for technical assistance.

Submitted: 18 August 2004
Accepted: 15 October 2004

References

Andrade, M.A., C. Perez-Iratxeta, and C.P. Ponting. 2001. Protein repeats: structures, functions, and evolution. *J. Struct. Biol.* 134:117–131.

Bailer, S.M., C. Balduf, and E. Hurt. 2001. The Nsp1p carboxy-terminal domain is organized into functionally distinct coiled-coil regions required for assembly of nucleoporin subcomplexes and nucleocytoplasmic transport. *Mol. Cell. Biol.* 21:7944–7955.

Belgareh, N., G. Rabut, S.W. Bai, M. van Overbeek, J. Beaudouin, N. Daigle, O.V. Zatsepina, F. Pasteau, V. Labas, M. Fromont-Racine, et al. 2001. An evolutionarily conserved NPC subcomplex, which redistributes in part to kinetochores in mammalian cells. *J. Cell Biol.* 154:1147–1160.

Boehmer, T., J. Enninga, S. Dales, G. Blobel, and H. Zhong. 2003. Depletion of a single nucleoporin, Nup107, prevents the assembly of a subset of nucleoporins into the nuclear pore complex. *Proc. Natl. Acad. Sci. USA.* 100:981–985.

Brunger, A.T., P.D. Adams, G.M. Clore, W.L. DeLano, P. Gros, R.W. Grosse-Kunstleve, J.S. Jiang, J. Kuszewski, M. Nilges, N.S. Pannu, et al. 1998. Crystallography & NMR system: A new software suite for macromolecular structure determination. *Acta Crystallogr. D Biol. Crystallogr.* 54: 905–921.

Collaborative Computational Project Number. 1994. The CCP4 suite: programs for protein crystallography. *Acta Crystallogr. D. Biol. Crystallogr.* 50: 760–763.

Chook, Y.M., and G. Blobel. 2001. Karyopherins and nuclear import. *Curr. Opin. Struct. Biol.* 11:703–715.

Cronshaw, J.M., A.N. Krutchinsky, W. Zhang, B.T. Chait, and M.J. Matunis. 2002. Proteomic analysis of the mammalian nuclear pore complex. *J. Cell Biol.* 158:915–927.

de la Fortelle, E., and G. Bricogne. 1997. Maximum-likelihood heavy-atom parameter refinement in the multiple isomorphous replacement and multiwavelength anomalous diffraction methods. *In* Methods in Enzymology, Macromolecular Crystallography. Vol. 276. R.M. Sweet and C.W. Carter Jr., editors. Academic Press Inc., New York. 472–494.

Devos, D., S. Dokudovskaya, F. Alber, R. Williams, B.T. Chait, A. Sali, and M.P. Rout. 2004. Components of coated vesicles and nuclear pore complexes share a common molecular architecture. *PLoS Biol.* doi: 10.1371/journal.pbio.0020380

Doublie, S. 1997. Preparation of selenomethionyl proteins for phase determination. *Methods Enzymol.* 276:523–530.

Doye, V., R. Wepf, and E.C. Hurt. 1994. A novel nuclear pore protein Nup133p with distinct roles in poly(A)+ RNA transport and nuclear pore distribution. *EMBO J.* 13:6062–6075.

Dunker, A.K., C.J. Brown, J.D. Lawson, L.M. Iakoucheva, and Z. Obradovic. 2002. Intrinsic disorder and protein function. *Biochemistry.* 41:6573–6582.

Favreau, C., H.J. Worman, R.W. Wozniak, T. Frappier, and J.C. Courvalin. 1996. Cell cycle-dependent phosphorylation of nucleoporins and nuclear pore membrane protein Gp210. *Biochemistry.* 35:8035–8044.

Galy, V., I.W. Mattaj, and P. Askjaer. 2003. *Caenorhabditis elegans* nucleoporins Nup93 and Nup205 determine the limit of nuclear pore complex size exclusion in vivo. *Mol. Biol. Cell.* 14:5104–5115.

Griffis, E.R., N. Altan, J. Lippincott-Schwartz, and M.A. Powers. 2002. Nup98 is a mobile nucleoporin with transcription-dependent dynamics. *Mol. Biol. Cell.* 13:1282–1297.

Harel, A., A.V. Orjalo, T. Vincent, A. Lachish-Zalait, S. Vasu, S. Shah, E. Zimmerman, M. Elbaum, and D.J. Forbes. 2003. Removal of a single pore subcomplex results in vertebrate nuclei devoid of nuclear pores. *Mol. Cell.* 11:853–864.

Hodel, A.E., M.R. Hodel, E.R. Griffis, K.A. Hennig, G.A. Ratner, S. Xu, and M.A. Powers. 2002. The three-dimensional structure of the autoproteolytic, nuclear pore-targeting domain of the human nucleoporin Nup98. *Mol. Cell.* 10:347–358.

Loiodice, I., A. Alves, G. Rabut, M. Van Overbeek, J. Ellenberg, J.B. Sibarita, and V. Doye. 2004. The entire Nup107-160 complex, including three new members, is targeted as one entity to kinetochores in mitosis. *Mol. Biol. Cell.* 15:3333–3344.

Lutzmann, M., R. Kunze, A. Buerer, U. Aebi, and E. Hurt. 2002. Modular self-assembly of a Y-shaped multiprotein complex from seven nucleoporins. *EMBO J.* 21:387–397.

Macaulay, C., E. Meier, and D.J. Forbes. 1995. Differential mitotic phosphorylation of proteins of the nuclear pore complex. *J. Biol. Chem.* 270:254–262.

Marcotte, E.M., M. Pellegrini, T.O. Yeates, and D. Eisenberg. 1999. A census of protein repeats. *J. Mol. Biol.* 293:151–160.

Miele, A.E., P.J. Watson, P.R. Evans, L.M. Traub, and D.J. Owen. 2004. Two distinct interaction motifs in amphiphysin bind two independent sites on the clathrin terminal domain beta-propeller. *Nat. Struct. Mol. Biol.* 11: 242–248.

Paoli, M. 2001. Protein folds propelled by diversity. *Prog. Biophys. Mol. Biol.* 76:103–130.

Pemberton, L.F., M.P. Rout, and G. Blobel. 1995. Disruption of the nucleoporin gene NUP133 results in clustering of nuclear pore complexes. *Proc. Natl. Acad. Sci. USA.* 92:1187–1191.

Rout, M.P., J.D. Aitchison, A. Suprapto, K. Hjertaas, Y. Zhao, and B.T. Chait. 2000. The yeast nuclear pore complex: composition, architecture, and transport mechanism. *J. Cell Biol.* 148:635–651.

Suntharalingam, M., and S.R. Wente. 2003. Peering through the pore: nuclear pore complex structure, assembly, and function. *Dev. Cell.* 4:775–789.

ter Haar, E., A. Musacchio, S.C. Harrison, and T. Kirchhausen. 1998. Atomic structure of clathrin: a beta propeller terminal domain joins an alpha zigzag linker. *Cell.* 95:563–573.

ter Haar, E., S.C. Harrison, and T. Kirchhausen. 2000. Peptide-in-groove interactions link target proteins to the beta-propeller of clathrin. *Proc. Natl. Acad. Sci. USA.* 97:1096–1100.

Walther, T.C., A. Alves, H. Pickersgill, I. Loiodice, M. Hetzer, V. Galy, B.B. Hulsmann, T. Kocher, M. Wilm, T. Allen, et al. 2003. The conserved Nup107-160 complex is critical for nuclear pore complex assembly. *Cell.* 113:195–206.

Weeks, C.M., and R. Miller. 1999. The design and implementation of SnB v2.0. *Journal of Applied Crystallography.* 32:120–124.

Yaseen, N.R., and G. Blobel. 1999. GTP hydrolysis links initiation and termination of nuclear import on the nucleoporin nup358. *J. Biol. Chem.* 274: 26493–26502.